Hindawi
Advances in Civil Engineering
Volume 2018, Article ID 5172878, 13 pages
https://doi.org/10.1155/2018/5172878

Research Article

Effect of Adjacent Hole on the Blast-Induced Stress Concentration in Rock Blasting

Yuezong Yang,[1,2] Zhushan Shao ,[1] Junfeng Mi,[3] and Xiaofeng Xiong[3]

[1]*School of Civil Engineering, Xi'an University of Architecture and Technology, Xi'an 710055, China*
[2]*School of Naval Architecture, Ocean and Civil Engineering, Shanghai Jiao Tong University, Shanghai 200240, China*
[3]*The 1st Engineering Co., Ltd. of China Railway 12th Bureau Group, Xi'an 710038, China*

Correspondence should be addressed to Zhushan Shao; shaozhushan@xauat.edu.cn

Received 24 April 2018; Accepted 18 September 2018; Published 15 November 2018

Guest Editor: Fengqiang Gong

To investigate the effect of an adjacent hole on the blast-induced stress concentration in rock blasting, a rock blasting model with an adjacent hole is explored through theoretical analysis and numerical simulation. The commercial software LS-DYNA is utilized to simulate adjacent hole effect in rock blasting, in which the Johnson–Holmquist concrete material model is used to simulate rock and the high-explosive-burn-explosive and the equation of state of JWL are used to simulate explosive. Influences of the key parameters of adjacent hole effect in rock blasting, pitch of holes, adjacent hole diameter, and uncoupled medium in a blasting hole are extensively explored. According to the simulation results, when the explosion stress wave spreads to the adjacent hole wall, the tangential stress on the adjacent hole wall induced by the explosion stress wave is always greater than the radial stress. Adjacent hole diameter has a major effect on stress concentration, but with the adjacent hole diameter increasing, the stress concentration phenomenon weakens and the free surface effect of the adjacent hole plays a more important role.

1. Introduction

With the continuous development of the national economy, more and more mining and tunnel projects are being constructed in China. Under some ideal conditions, mechanized excavation has the advantages of speediness and low impact on the environment [1, 2]. But under unstable ground and complex geological conditions, mechanized excavation, compared with drilling and blasting, is inefficient and poor adaptability. Especially in hard rock, the wear of cutting tools of the excavating equipment is severe and the removal and reinstallation of cutting tools takes a long time, so mechanized excavation in hard rock is uneconomic and time-consuming. Although drilling and blasting is a traditional excavation method, it still plays an important role in tunnel excavation on account of its good applicability and economy [3–5]. At present, the mainstream blasting method is controlled blasting, which includes directional blasting, smooth blasting, splitting blasting, and millisecond blasting [6–8]. In the process of engineering blasting, explosive detonation is an instantaneous chemical reaction with tremendous energy release, which triggers effective vibration to break the rock.

Setting empty holes near the blasting hole is a valid way for directional blasting. When explosive detonates in the blasting hole, the adjacent empty hole close to the blasting hole not only can provide free face for rock deformation but also can change stress distribution in rocks around the empty hole. After explosive detonates, blasting-induced shock waves act on the blasting hole wall in the first place, activating randomly primary fissures and fresh fissures in the rock near the blasting hole, and then outspread across external rock [9, 10]. The pressure on the blast hole wall generally exceeds the dynamic compressive strength of the rock, making the rock mass to deform plastically and forming the crushed zone [11–13]. Because the production of crushed zone consumes a tremendous amount of explosive energy, compressive shock waves turn into compressive stress waves after passing this zone. When the stress waves propagate to the adjacent empty hole wall,

compressive stress waves turn into tension stress wave due to reflection on empty hole wall [14–16]. If reflected tension stress waves exceed the dynamic tension strength of the rock, fissure will arise [17, 18]. Because of the induction effect of the empty hole, blasting-induced rock fracture will propagate towards the empty hole, which is called as empty hole effect. Due to the complexity and instantaneity of explosive load, the crack propagation law in rock with empty hole is still unclear. Therefore, it is of great significance to study the mechanism of the empty hole in rock blasting and its interaction with blasting-induced cracks.

Experimental studies of rock blasting are very expensive and time-consuming [16]. It has been shown that theoretical research and numerical simulation can serve as an efficient approach to reveal the crack propagation law in rock blasting [19–22]. In this research, the following topics are discussed by the methods of theoretical research and numerical simulation: (a) the influence of the pitch of holes on the crack propagation law, (b) the influence of the adjacent empty hole diameter on the crack propagation law, and (c) the effect of uncoupled medium on blasting load acting on blasting hole wall. These research results have reference value in selecting blasting parameters.

2. Theoretical Research of the Effect of Adjacent Empty Hole

2.1. The Stress Concentration Effect of Adjacent Empty Hole. When an explosive is detonated, the impact load generated by explosive explosion creates a shock stress field in the rock. In the rock around the blasting hole, the impact load acts on it and creates pressure, which can be expressed as

$$P_0 = \frac{1}{1+\gamma}\rho_0 D_V^2, \tag{1}$$

where P_0 is the pressure on the blasting hole wall generated by the shock wave, ρ_0 is the explosive density, D_v is the explosive velocity, and γ is the exponent of adiabatic expansion of the detonation gas.

Based on the principle of wave's transmission and reflection, the pressure created by the shock wave transmitting into the rock can be expressed as

$$P = \frac{2\rho c_p}{\rho c_p + \rho_0 D_V} P_0, \tag{2}$$

where c_p is the acoustic wave speed in the rock and ρ is the rock density.

After shock waves transmit across the interface between explosion and rock, it will spread along the outer rock. With the increase of distance, shock waves translate into stress waves in no time. The stress waves' peaks decrease as follows:

$$\sigma_r = P\left(\frac{r_1}{r}\right)^{\alpha}, \qquad \sigma_\theta = b\sigma_r, \tag{3}$$

where σ_r is the radial stress at a point in the rock, σ_θ is the tangential stress at a point in the rock, P is the pressure created by the shock wave transmitting in the rock, r_1 is the blasting hole diameter, r is the distance between a point in the rock and the center of the blasting hole, and α is the attenuation coefficient in the rock, which can be expressed as

$$\alpha = 2 - \frac{\mu_d}{1-\mu_d}, \tag{4}$$

where μ_d is the dynamic Poisson ratio of the rock. It has been revealed by correlational researches that the dynamic Poisson ratio is in correlation with the rock strain rate [23–25]. With the increase of the rock strain rate, the dynamic Poisson ratio of rock will decrease. In the loading rate range of engineering blasting, the relation between the dynamic Poisson ratio and the static Poisson ratio can be expressed as

$$\mu_d = 0.8\mu, \tag{5}$$

where μ is the static Poisson ratio of rock.

The researches about the physical process of rock blasting show that the attenuation of the explosive stress wave is not only related to the physical mechanical properties of the rock but also depends on the explosive detonation parameters [26–28]. Effects of explosive detonation parameters on stress not only reflect on the pressure on blasting hole wall but also on the stress wave attenuation coefficient. So far, the certain way to determine the attenuation coefficient of stress wave propagation has not been understood completely.

When the stress wave reaches empty hole wall, the stress near the empty hole wall is greater than that of the rock without hole due to the stress concentration phenomenon. On the basis of elastic mechanics theory [29], the peak stress near the empty hole wall can be expressed as

$$\begin{aligned}
\sigma_{rr} &= \frac{1}{2}\left[\left(1-k^2\right)\left(\sigma_\theta - \sigma_r\right) + \left(1-4k^2+3k^4\right)\left(\sigma_\theta \cos 2\theta + \sigma_r \cos 2\theta\right)\right],\\
\sigma_{\theta\theta} &= \frac{1}{2}\left[\left(1+k^2\right)\left(\sigma_\theta - \sigma_r\right) + \left(1+3k^2\right)\left(\sigma_\theta \cos 2\theta + \sigma_r \cos 2\theta\right)\right],\\
\tau_{r\theta} &= \frac{1}{2}\left[\left(1+2k^2-3k^4\right)\left(\sigma_\theta \cos 2\theta + \sigma_r \cos 2\theta\right)\right],\\
k &= \frac{r_B}{r_2},
\end{aligned} \tag{6}$$

where σ_{rr} is the radial stress in adjacent rock around the empty hole, $\sigma_{\theta\theta}$ is the tangential stress in adjacent rock around the empty hole, $T_{r\theta}$ is the shearing stress in adjacent rock around the empty hole, r_2 is the empty hole radius, r is the distance between a point in the rock and the center of the empty hole, and θ is the angle between the ligature of the calculated point and blasting hole and the ligature of the blasting hole and the empty hole, as shown in Figure 1. The stress state on the empty hole wall is that $\sigma_{rr} = 0, T_{r\theta} = 0$, and

$$\sigma_{\theta\theta} = \left(\sigma_\theta - \sigma_r\right) + 2\left(\sigma_\theta \cos 2\theta + \sigma_r \cos 2\theta\right). \tag{7}$$

By taking the derivative of $\sigma_{\theta\theta}$, we can get $d\sigma_{\theta\theta}/d\theta = -4\sin 2\theta(\sigma_\theta + \sigma_r)$. When $d\sigma_{\theta\theta}/d\theta = 0$, that is, $\theta = \pm\pi$, we can get the peaks of tensile stresses, which can be expressed as

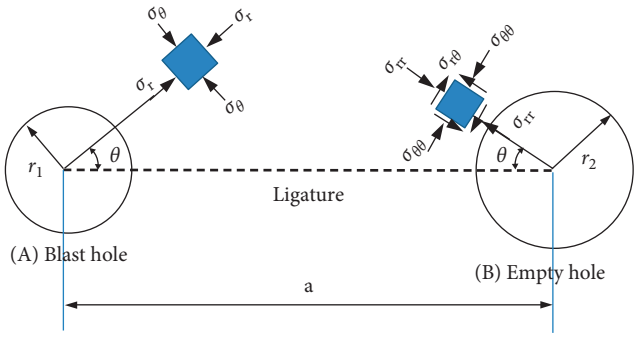

Figure 1: The stress concentration effect of an adjacent empty hole.

$$\sigma_{\theta\theta} = 3\sigma_\theta + \sigma_r = (3b+1)P\left(\frac{r_1}{a-r_2}\right)^\alpha. \tag{8}$$

The empty hole can make tensile stress along the ligature between the blasting hole and the empty hole to be the maximal tensile stress in all tensile stresses at the same distance from the blasting hole [30].

2.2. The Free Surface Effect of Adjacent Empty Hole. When the stress wave propagates to the empty hole wall, the stress wave, which is incident wave, will reflect and transmit in the boundary of rocks and air, causing reflected wave in rock and transmitted wave in air. The reflected waves impact on rock and make rock fracture. The following analysis focuses the reflection regularity of stress wave when it propagates vertically to the empty hole wall.

As shown in Figure 2, the wave impedance of rock is $\rho_{r0}C_{r0}$, in which ρ_{r0} is the rock density and C_{r0} is the speed of wave propagation in the rock. The wave impedance of air is $\rho_{a0}C_{a0}$, in which ρ_{a0} is the air density and C_{a0} is the speed of wave propagation in air. According to the conservation of momentum, the particle velocity increment on boundary of rock and air can be expressed as

$$\begin{aligned} u_I &= \frac{\sigma_I}{\rho_{r0}C_{r0}}, \\ u_R &= -\frac{\sigma_R}{\rho_{r0}C_{r0}}, \\ u_T &= \frac{\sigma_T}{\rho_{a0}C_{a0}}, \end{aligned} \tag{9}$$

where u_I is the velocity increment of rock particle caused by incident waves, u_R is the velocity increment of rock particle caused by reflected waves, u_T is the velocity increment of air particle in the empty hole, σ_I is the intensity of the incident wave, σ_R is the intensity of the reflected wave, and σ_T is the intensity of the transmitted wave.

The stress and particle velocity on the boundary surface meets the continuous condition, and this can be expressed as

$$\sigma_I + \sigma_R = \sigma_T, \tag{10}$$

$$u_I + u_R = u_T. \tag{11}$$

Considering Equations (10–12), we can get

$$\begin{aligned} \sigma_R &= F\sigma_I, \\ u_R &= Fu_I, \\ \sigma_T &= T\sigma_I, \\ u_T &= \left(\frac{\rho_{r0}C_{r0}}{\rho_{a0}C_{a0}}\right)Tu_I, \end{aligned} \tag{12}$$

where F and T are called the reflection coefficient and transmission coefficient, respectively, whose values are determined by the wave impedance of the rock and air, which can be expressed as

$$\begin{aligned} F &= \frac{\rho_{a0}C_{a0} - \rho_{r0}C_{r0}}{\rho_{a0}C_{a0} + \rho_{r0}C_{r0}}, \\ T &= \frac{2\rho_{a0}C_{a0}}{\rho_{a0}C_{a0} + \rho_{r0}C_{r0}}, \\ T &= 1 + F. \end{aligned} \tag{13}$$

Because air density is much smaller than rock density, that is $\rho a0/\rho k0 = 0$, so $F = -1$ and $T = 0$. When compression wave spreads to a free surface and reflects, the compression wave changes into a tensile wave, and then, tensile wave acts on rock. Because the tensile strength of the rock medium is much lower than the shear strength and compressive strength of the rock, the reflected tensile wave coming from the empty hole wall has an important effect on breaking rock. With the adjacent empty hole diameter increasing, more stretching wave is reflected into the rock medium, as shown in Figure 3, and it is helpful for rock breaking.

3. ANSYS/LS-DYNA Algorithm and Material Constitutive Model

3.1. ANSYS/LS-DYNA Algorithm. There are a variety of algorithms to simulate the explosion process in ANSYS/LS-DYNA. The explosion of dynamite in rock is accompanied with the intrusion of explosive gas, which acts as a gas wedge for crack expansion. The key of blasting simulation is to realize the interaction between rock mass and dynamite.

For Lagrange algorithm, materials cannot flow in the grid, and the finite element mesh in this algorithm can become deformed seriously so that this algorithm cannot solve blasting problem. The Euler algorithm allows the material flowing in the fixed grid. We can make Euler finite element mesh couple with Lagrange finite element mesh to deal with the fluid-structure interaction under different conditions. However, in the Euler algorithm, in order to accurately capture the coupling deformation of gas and rock material in the explosion, the fine partitioning of the grid is required, resulting in the increase of the computational cost and the consumption of a large number of machines. The ALE algorithm combines the advantages of Lagrange algorithm and Euler algorithm. In the calculating order of the ALE method, Lagrange calculation is performed firstly and

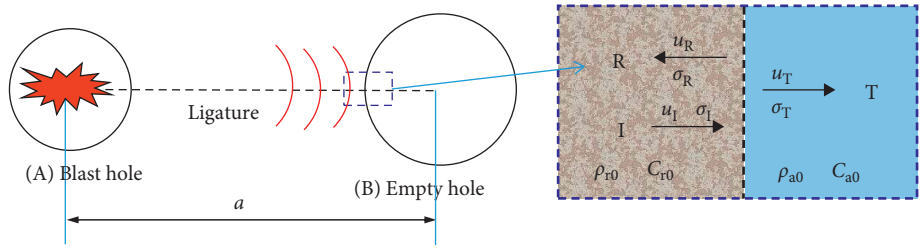

Figure 2: The free surface effect of an adjacent empty hole.

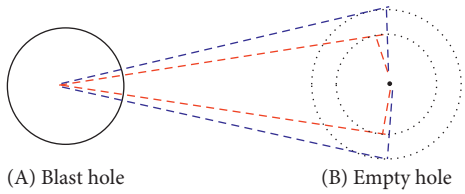

Figure 3: The influence of adjacent empty hole diameter.

then the grid deforms with the deformation of the material. In contrast, the ALE algorithm is more suitable for solving the problem of large deformation caused by blasting [31]. Therefore, the ALE algorithm and its fluid-structure coupling method are selected to simulate rock blasting in the subsequent chapters.

3.2. Rock Constitutive Model. In order to study the deformation and failure mechanism of rock material under dynamic load, many scholars have established lots of rock constitutive models [32, 33]. In blasting simulation, Johnson–Holmquist concrete material model is representative, which can describe the high strain and large deformation of rock and concrete materials under dynamic load more accurately [34–36]. The equivalent yield strength of the JHC model is a function of the pressure strain rate and damage factor. Meanwhile, pressure is a function of volume strain, and damage accumulation is a function of plastic volume strain, equivalent plastic strain, and pressure. The intensity of the JHC model is described by the normalized equivalent stress:

$$\sigma^* = \left[A(1-D) + \mathrm{BP}^{*N}\right]\left(1 + C\ln\dot{\varepsilon}^*\right), \tag{14}$$

where $\sigma^* = \sigma/f_c'$ is the ratio of the actual equivalent stress σ to the static compressive strength f_c', $P^* = P/f_c'$ is the dimensionless pressure, where P is the unit hydrostatic pressure, $\dot{\varepsilon}^* = \dot{\varepsilon}/\dot{\varepsilon}_0$ is the dimensionless strain rate, where $\dot{\varepsilon}$ is the true strain rate and $\dot{\varepsilon}_0$ is the reference strain rate, A is the standardized cohesion strength, B is the normalized pressure hardening coefficient, N is the pressure hardening index, and C is the strain rate coefficient.

The damage factor $D(0 \le D \le 1)$ can be obtained by equivalent plastic strain and plastic volume strain as

$$D = \sum \frac{\Delta\varepsilon_P + \Delta\mu_P}{\varepsilon_P^f + \mu_P^f}\Delta\varepsilon_p\varepsilon, \tag{15}$$

where $\Delta\varepsilon_P$ is the equivalent plasticity, $\Delta\mu_P$ is the equivalent volume strain increment, $\varepsilon_P^f + \mu_P^f = D_1(P^* + T^*)^{D_2}$ is the plastic strain at normal pressure P, ε_P^f is the equivalent plastic strain, μ_P^f is the equivalent volume strain, $T^* = T/f_c'$ is the maximum tensile strength of the material, T is the tensile strength of the material, and D_1 and D_2 are damage constants.

The related parameters of the rock constitutive model are shown in Table 1.

3.3. Explosive Material Model. The key to study the blasting is to determine the blasting load. The blasting damage on rock can be quantitatively analyzed by determining the pressure change course curve in the blasting hole. In actual measurement, the high temperature and high pressure makes it difficult to measure the pressure change of the blast hole. The explosive constitutive model provided by numerical simulation technology can effectively solve this obstacle. For the complex characteristics of explosive detonation, the dynamite constitutive model provided in LS-DYNA can accurately describe the physical and chemical properties of explosives. In this paper, the MAT-high-explosive-burn-explosive embedded in the LS-DYNA program is selected as the explosive model. The relationship between pressure and volume change of detonation product is described by using the JWL state equation. The state equation of JWL is described as follows:

$$P = A\left(1 - \frac{\omega}{R_1V}\right)e^{-R_1V} + B\left(1 - \frac{\omega}{R_2V}\right)e^{-R_2V} + \frac{\omega E_0}{V}, \tag{16}$$

where P is the pressure of detonation product, V is the relative volume, E_0 is the initial internal energy density, and A, B, R_1, R_2, and ω are constants.

The related parameters of the explosive material model are shown in Tables 2 and 3.

3.4. Air and Water Constitutive Model. In LS-DYNA, air and water are treated as fluid materials. Fluid materials generally need to be described in two aspects: constitutive equation and state equation. The former describes the relation between stress and strain and the latter describes the relationship between volume deformation and pressure. In the calculation of fluid-structure interaction, the NULL material is adopted as the constitutive equation and the Gruneisen equation is adopted as the state equation:

Table 1: Rock material parameter.

R_0 (g·cm^{-3})	G (GPa)	A	B	C	N	F_C (GPa)	T (GPa)	EPS_0	EF_{MIN}
2.44	14.86	0.79	1.60	0.007	0.61	0.048	0.004	$1 * 10^{-6}$	0.01
SF_{MAX}	P_C	U_C	P_L (GPa)	U_L	D_1	D_2	K_1	K_2 (GPa)	K_3 (GPa)
7	0.016	0.001	0.8	0.1	0.04	1	85	−171	208

Table 2: High-explosive-burn parameter.

R_0 (g·cm^3)	D (m·s^{-1})	PCJ (MPa)	K	G	SIGY
1.64	6930	$0.27 * 10^5$	0	0	0

Table 3: Parameters of the state equation of dynamite JWL.

A (GPa)	B (GPa)	R_1	R_2	ω	E (GPa)	V_0
374	3.23	4.15	0.95	0.3	7	1

$$P = \frac{\rho_0 C^2 \left[1 + (1 - \gamma_0/2)\mu - (a/2)\mu^2\right]}{\left[1 - (S_1 - 1)\mu - S_2(\mu^2/\mu + 1) - S_3\left(\mu^3/(\mu + 1)^2\right)\right]^2}, \tag{17}$$

where ρ_0 is the material density, γ_0 is the Gruneisen parameter, E_0 is the internal energy, C is the intercept of a curve, S_1, S_2, and S_3 are coefficients of the slope of the curve, and a is the first-order volume correction of γ_0 and μ.

4. The Effect of Pitch of Holes on Stress Concentration

4.1. Calculation Model. In rock blasting, the empty hole effect only plays a role within a certain range around the blasting hole, and the empty hole effect will not be obvious beyond the range. This paper establishes a numerical model to analyze the effect of pitch of holes on empty hole effect. As shown in Figure 4, the model size is 150 cm × 150 cm, the blasting hole whose diameter is 5 cm is placed in the center of the model with a coupling charge, and the diameter of empty hole is 5 cm. The distance between blasting hole and empty hole is a. According to the difference of the hole spacing a, 4 sets of comparison simulation tests were set up. In Table 4, r_1 is the blasting hole radius and r_2 is the empty hole radius.

4.2. Result and Analysis. Taking model 1 as an example, the explosive load acts on hole wall after the detonation of the explosive in the blasting hole, and the explosion stress wave propagates from the center of the blasting hole to the surrounding rock, as shown in Figure 5(a). In the initial stage of the explosion stress wave propagating, the empty hole has no obvious guiding effect on the explosive stress wave propagating, and the explosion stress wave is centered at the center of the blasting hole and propagates outward in a circular shape. When the explosive stress wave spread around the empty hole, as shown in Figure 5(b), because of the existence of empty hole, explosion stress wave

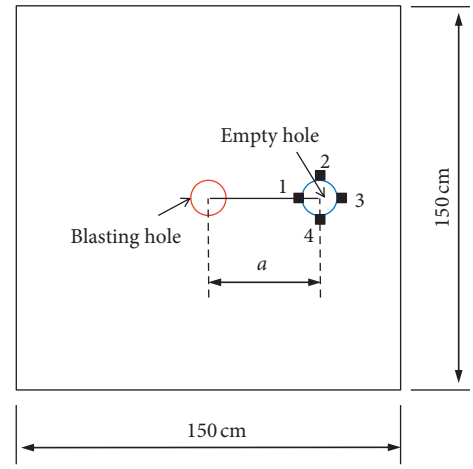

Figure 4: Comparison test of different distances between holes.

Table 4: Experimental group parameters of different distances between holes.

Number	r_1 (cm)	a (cm)	r_2 (cm)	$a/2r_1$
Model 1	2.5	25	2.5	5
Model 2	2.5	37.5	2.5	7.5
Model 3	2.5	50	2.5	10
Model 4	2.5	62.5	2.5	12.5

propagating law changes and stress concentration phenomenon appears on empty hole wall near the blasting hole.

Through the calculation results of different models with different pitches of holes, we can find that the damage degree of rock mass around the blast hole and empty hole is more serious than other areas. With the further propagation of the explosive stress wave, the effective stress on empty hole wall increases gradually, as shown in Figure 6. We can observe that there exists a small low-damage zone between the blasting and the empty hole. This phenomenon can be explained by the superposition of waves. When a cylindrical explosive is detonated in the blasting hole, the explosion stress wave propagates outwards in the form of compression wave. The adjacent empty hole wall can be considered as a free surface due to no constraints. When the explosion stress wave propagates to the empty hole wall, the explosion stress wave will reflect and change from compression wave to tension wave. The reflected stress wave will propagate to the blasting hole direction in the form of tension wave. The superposition of compression wave coming from the blasting hole and that of the tension wave coming from the empty hole will affect the damage distribution of rock mass. In the area where the compression wave strength is close to

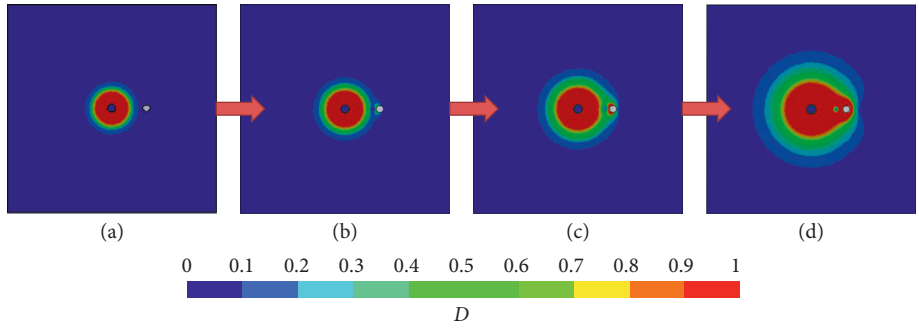

Figure 5: Damage evolution process of the model 1. (a) $t = 11.971\,\mu s$, (b) $t = 13.991\,\mu s$, (c) $t = 17.47\,\mu s$, and (d) $t = 24.482\,\mu s$.

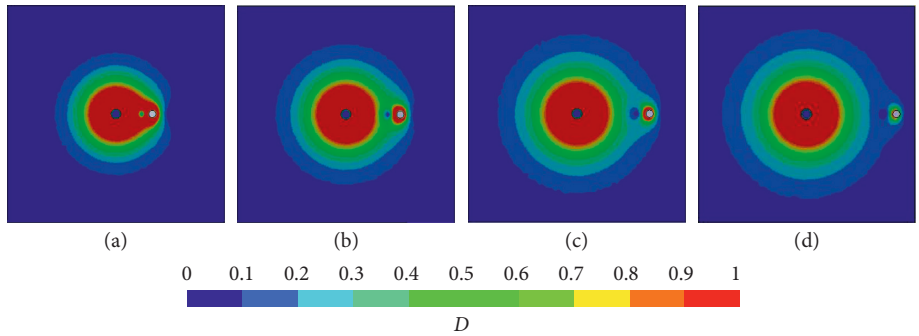

Figure 6: Damage evolution with different distances between two holes when $t = 25\,\mu s$. (a) $a/2r_1 = 5$, (b) $a/2r_1 = 7.5$, (c) $a/2r_1 = 10$, and (d) $a/2r_1 = 12.5$.

that of the tension wave, the compression wave can cancel out the tension wave, so that the damage degree in this area is very small.

In the stress analysis of finite element software ANSYS, positive stress is tensile stress and the negative stress is compressive stress. Through the comparison of radial stress and tangential stress of the empty hole wall, which can be found that tangential stress and radial stress are all compressive stress, as shown in Figure 7, and the tangential stress is greater than the radial stress, and the tangential stress peak is usually 3-4 times than the radial stress peak, as shown in Figure 8.

The stress wave produced by the explosion of the explosive in the blasting hole gradually propagates from the center of blasting hole to outside. The effect of stress wave on the empty hole wall is not obvious before it arrives at the empty hole. When the stress wave propagates to the empty hole, the radial stress and tangential stress of the empty hole wall increase sharply. In the initial stage of increasing stress, the growth law of radial stress and tangential stress is the same. After that, the radial stress decreases slightly, then stays the same and reaches the second peak after a period of time. At the same time, the tangential stress has been increasing, and at the time when the radial stress reached the second peak, it also reaches the peak. In the process of stress changing, the tangential stress is always greater than the radial stress.

Under the action of explosion stress wave, empty hole wall has displacement to the empty hole center due to the fact that empty hole wall has no restraint inside; i.e., the pore diameter is reduced. The displacements of the empty hole wall are not uniform, the displacement of point 1 is the biggest, the displacement of point 3 is the least, and the displacement of point 2 is equal approximately to that of point 4, as shown in Figures 9 and 10.

5. The Effect of the Adjacent Hole Diameter on Stress Concentration

5.1. Calculation Model. In rock blasting, when the empty hole diameter increases, the more tensile wave is reflected into the rock medium, and the more favorable for fracture extension in rock. It is helpful for enhancing free surface effect of empty hole to enlarge the empty hole diameter. In this paper, a numerical calculation model is established to analyze the effect of empty hole diameter on empty hole effect. As shown in Figure 11, the model size is 150 cm × 150 cm. The blasting hole with a diameter of 5 cm and coupling charge is placed in the center of the model. The empty hole was placed at the point which is 37.5 cm from the blasting hole center, and the radius r_2 was 1.25 cm, 2.5 cm, 3.75 cm, and 5 cm. According to the difference of the empty hole radius r_2, a total of 4 sets of comparison simulating tests were set up, whose parameters are shown in Table 5.

5.2. Result and Analysis. The plastic area around the empty hole increases as the empty hole radius increases, as shown

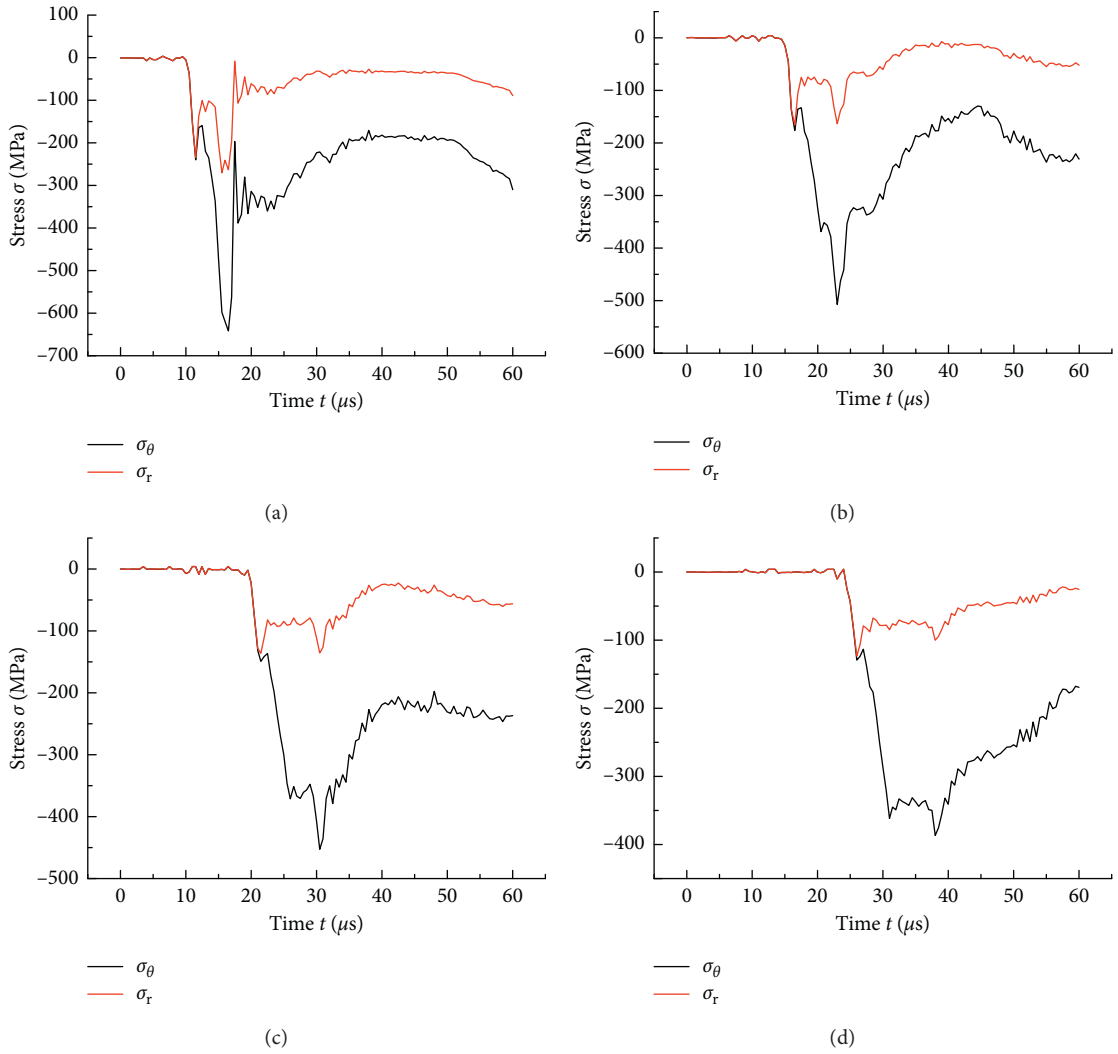

Figure 7: Contrast of radial stress and tangential stress on adjacent empty hole wall. (a) $a/2r_1 = 5$, (b) $a/2r_1 = 7.5$, (c) $a/2r_1 = 10$, and (d) $a/2r_1 = 12.5$.

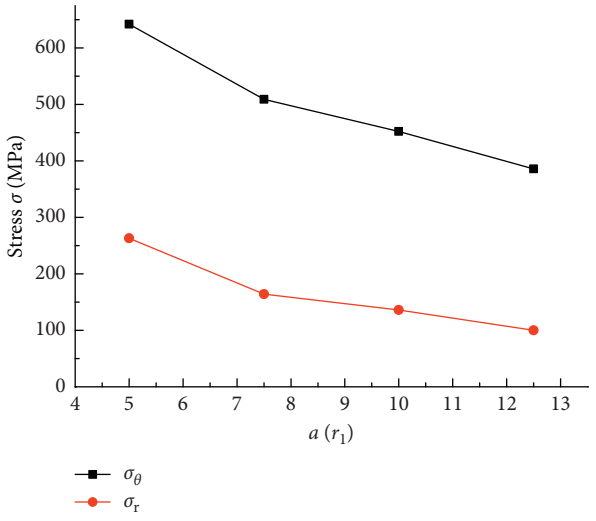

Figure 8: The peak stress on adjacent empty holes wall varies with the hole spacing.

in Figure 12. The high stress area around the empty hole has a tendency to move towards blasting hole. This indicates that with the empty hole diameter increasing, the stress concentration phenomenon weakens, and the free surface effect of empty hole plays a major role.

In order to analyze the stress distribution of the empty hole wall, point 1 and point 2 are selected, which are the nearest and the farthest points to the blasting hole, as shown in Figure 11. The growth of effective stress at point 2 lags behind that of point 1, as shown in Figure 13. When empty hole diameter is smaller than the blasting hole, although the effective stress on point 1 begins to increase earlier than point 2, the effective stress growth law sand effective peak values of point 1 and point 2 are the same. With the increase of the empty hole diameter, the time interval of effective stress between point 2 and point 1 increases. When empty hole diameter is bigger than the blasting hole, the effective stress of point 1 has obvious crest and effective stress change of point 2 is flat.

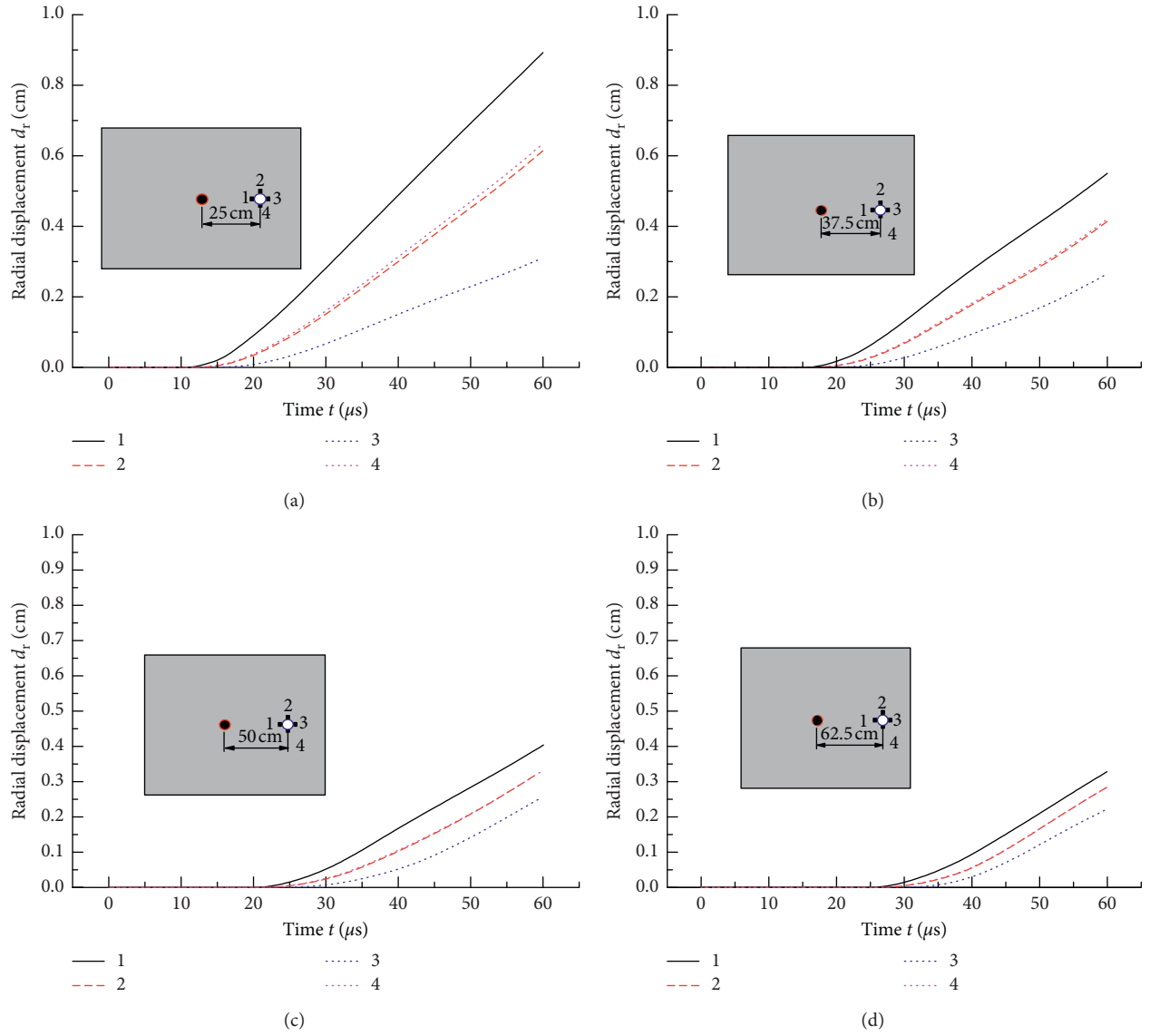

Figure 9: Radial displacement of adjacent empty holes wall with different hole spacing. (a) $a/2r_1 = 5$, (b) $a/2r_1 = 7.5$, (c) $a/2r_1 = 10$, and (d) $a/2r_1 = 12.5$.

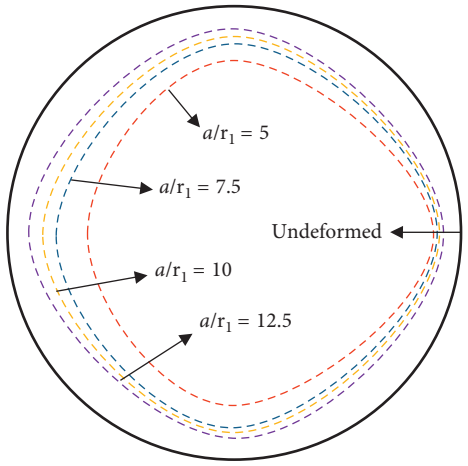

Figure 10: Adjacent empty hole deformation diagram with different hole spacing.

When the adjacent empty hole diameter is larger than the blasting hole diameter, the moment at which the effective stress begins to increase at the point 2 lags behind that of point 1, and with the increase of the adjacent empty hole diameter, the retardation time increases, as shown in Figure 14.

6. Comparison of Different Uncoupled Medium Charges

6.1. Calculation Model. There are two kinds of blasting hole charging mode: coupling charge and uncoupling charge. Due to the different coupling media, there are many kinds of uncoupling mode, and the modes that are commonly used are air-uncoupling charge and water-uncoupling charge. In the case of uncoupled charge blasting, the detonation wave and the detonation gas act on the uncoupling medium first.

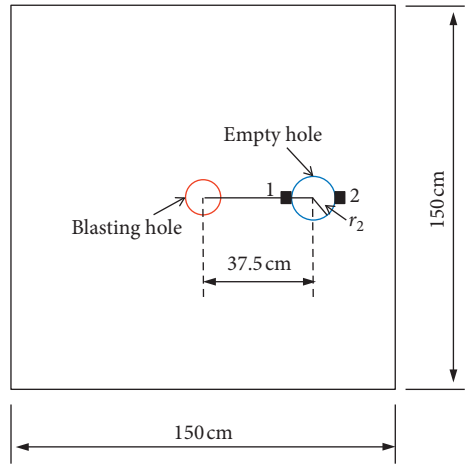

Figure 11: Comparison test of different adjacent empty hole radii.

Table 5: Experimental group parameters of different adjacent empty hole radii.

Number	r_1 (cm)	a (cm)	R_2 (cm)	r_2/r_1
Model 1	2.5	37.5	1.25	0.5
Model 2	2.5	37.5	2.5	1
Model 3	2.5	37.5	3.75	1.5
Model 4	2.5	37.5	5	2

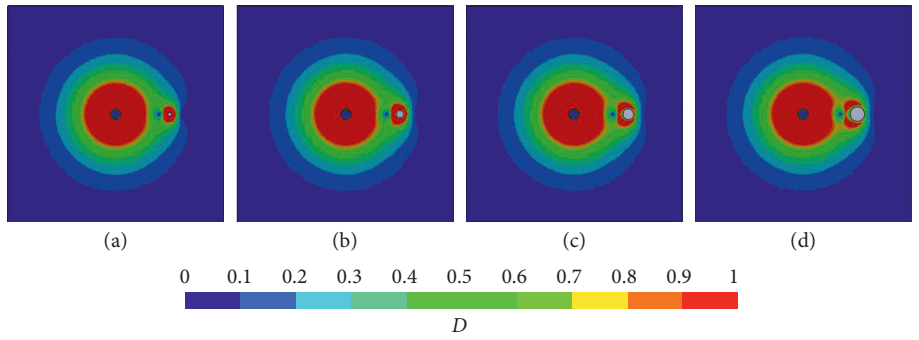

Figure 12: Damage distribution with different adjacent empty hole radii when $t = 25\,\mu$s. (a) $r_2/r_1 = 0.5$, (b) $r_2/r_1 = 1$, (c) $r_2/r_1 = 1.5$, and (d) $r_2/r_1 = 2$.

The load is then applied to the blast hole wall through the transmission of the uncoupled medium. The different uncoupling media have different performances and the way to transmit explosive energy is different, so the transmission pressure on the rock near blasting hole wall is very different. In the water-medium uncoupled charge, the detonation wave compresses water medium causing the shock wave in the water, which transmits to rock through water. Because of the cushion effect of water, the pressure on the blasting hole wall is reduced compared with coupling charge. In the air-medium uncoupled charge, because the compressibility of air is very strong, the detonation product expands to fill the blasting hole and then acts on the blasting hole wall, so the pressure on the blasting hole wall is also reduced compared with coupling charge. The different charging forms have great influence on pressure of blasting hole wall. In addition, the dynamic stress field in the surrounding rock is affected, which can affect the extent of blasting damage and destruction of rock.

Numerical simulation is used to reconstruct the stress wave during explosion, which is one kind of main methods to study blasting. In this paper, LS-DYNA numerical simulation platform is proposed to establish a single hole model of air-medium uncoupled charging blasting and water-medium uncoupled charging blasting, as shown in Figure 15, and the decouple coefficients of two models are all 1.5.

6.2. Result and Analysis. According to the explosive stress distribution and the dynamic compressive strength of the rock under the blasting load, we can simply regard the zone where the damage factor is greater than 0.9, the red area in Figure 16, as the crushed zone, the zone where the damage

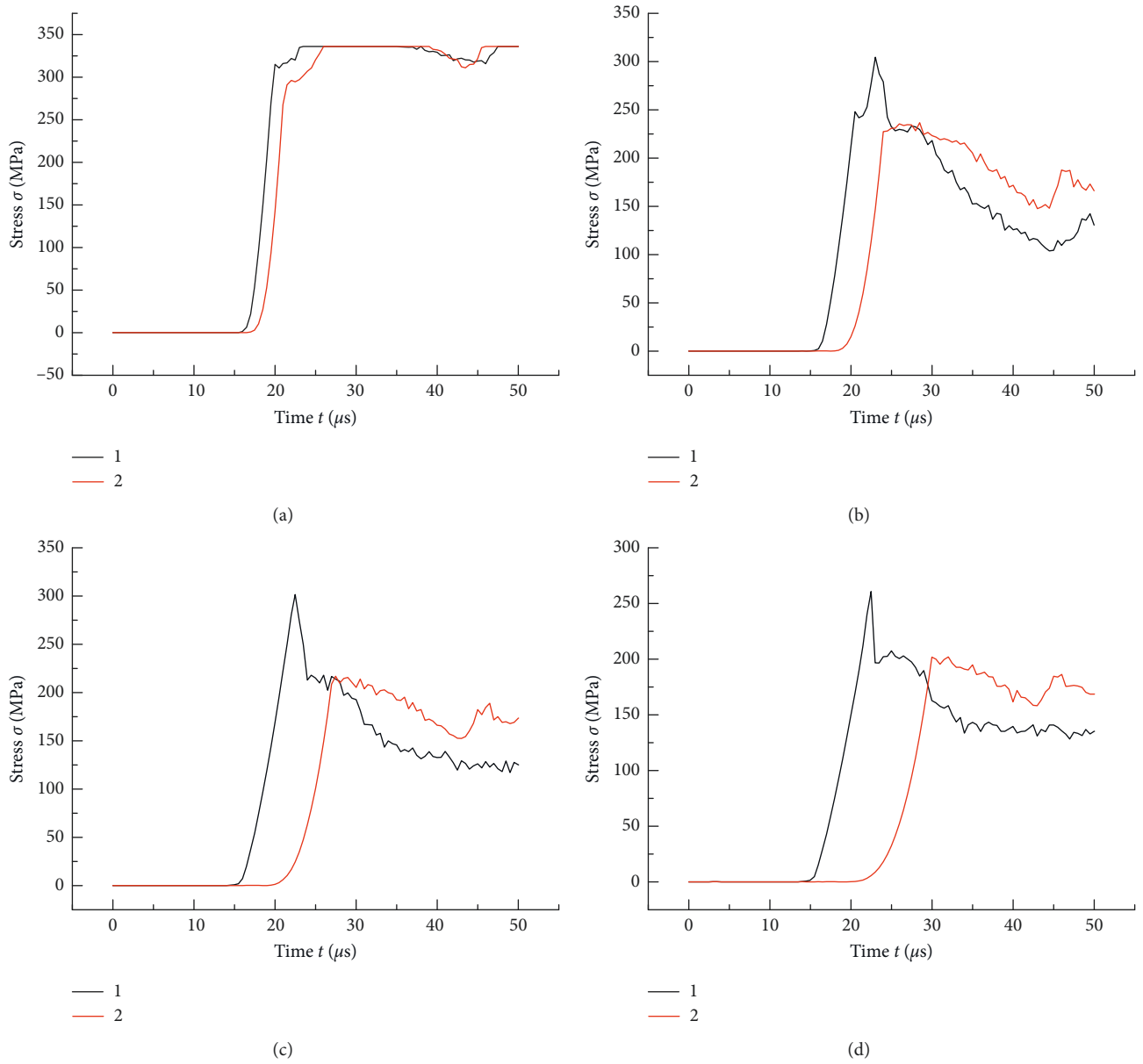

Figure 13: The effective stress change of point 1 and point 2 on empty hole wall.

factor is in the region of 0.1 to 0.9, which is green and shallow blue area in Figure 12, as a fracture zone, the zone where the damage factor is less than 0.1, which is the dark blue area in Figure 12, as the elastic zone. By comparing the rock mass damage distribution of coupling charge, air medium-uncoupling charging, and water-uncoupling charging, we can know that the crushing area produced by the water-medium uncoupled charging is basically the same as that produced by the coupling charging. The fracture zone produced by the water-medium uncoupled charging is greater than that of the coupling charging. The crushing zone and fracture zone of air-medium uncoupled charging are less than that of coupling charge and water medium. The blasting efficiency of the water-medium uncoupled charging is the highest, and the rock-breaking effect is the best, which is suitable for cut hole blasting. The damage to rock mass caused by air uncoupled charging is minimal. Air uncoupled charging can be used in peripheral eye blasting in smoothing blasting to reduce the damage to the surrounding rock.

After explosive detonation, the stress of the blasting hole wall rises to a maximum stress state in a very short time. In coupling charge, the blasting hole wall pressure reached the peak state of 13.08 GPa when it is 3.99 μs after the explosive explosion. In water-uncoupling charge, the blasting hole wall pressure reached the peak state of 11.72 GPa when it is 4.47 μs after the explosive explosion. In air-uncoupling charge, the blasting hole wall pressure reached the peak state of 5.16 GPa when it is 5.49 μs after the explosive explosion. As shown in Figure 17, the pressure of the blasting hole wall produced by coupling charge is the biggest. The blasting hole wall pressure caused by the water-uncoupling charge is slightly less than that of the coupling charge. The

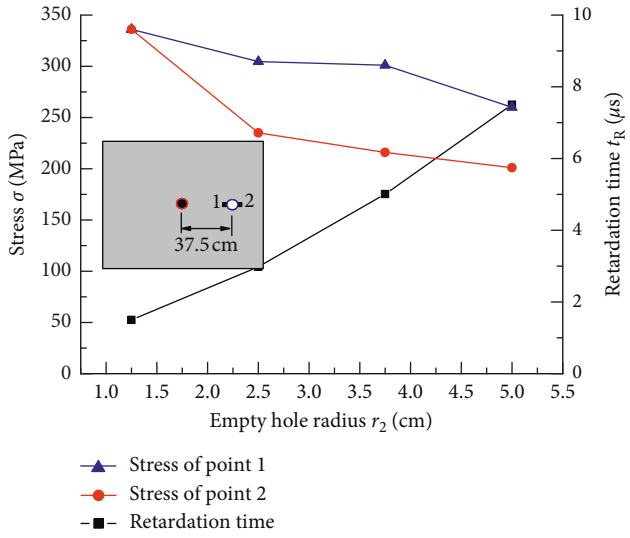

FIGURE 14: The stress of point 1 and point 2 on empty hole wall.

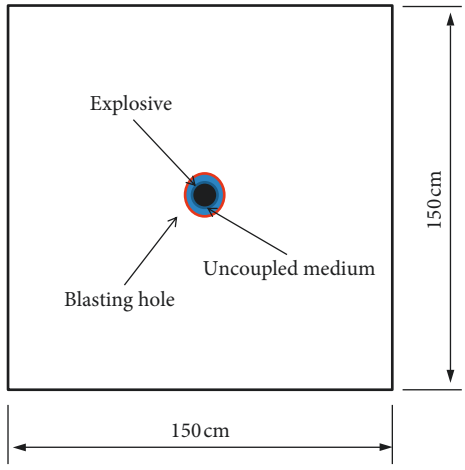

FIGURE 15: Comparison test of different uncoupling media.

blasting hole wall pressure generated by the air-uncoupling charge is 0.4 times the pressure of the blasting hole wall produced by the coupling charge, as shown in Figure 18. By comparing the time of blasting hole wall pressure reaching peak value, it is known that the air medium has a better cushioning effect on the blast wave than the water medium.

Comparing the stress in the surrounding rock with three kinds of charging methods, coupling charge, water-uncoupling charge, and air-uncoupling charge, we can find that the stress in the surrounding rock with the three charging methods all decreases exponentially with the distance. The stress produced by coupling charge and water-uncoupling charge is greater than that of air-uncoupling charge on blasting hole wall and in the surrounding rock. The stresses with the three kinds of loading methods are consistent beyond 15 cm, as shown in Figure 18.

7. Conclusion

In the present study, LS-DYNA is used to simulate the effect of adjacent empty hole. The influences of key parameters of

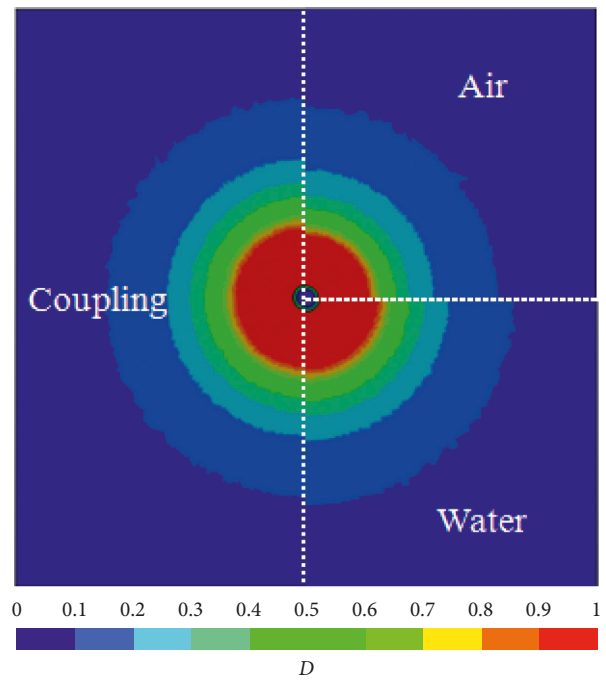

FIGURE 16: The rock mass damage degree comparison with different uncoupling media.

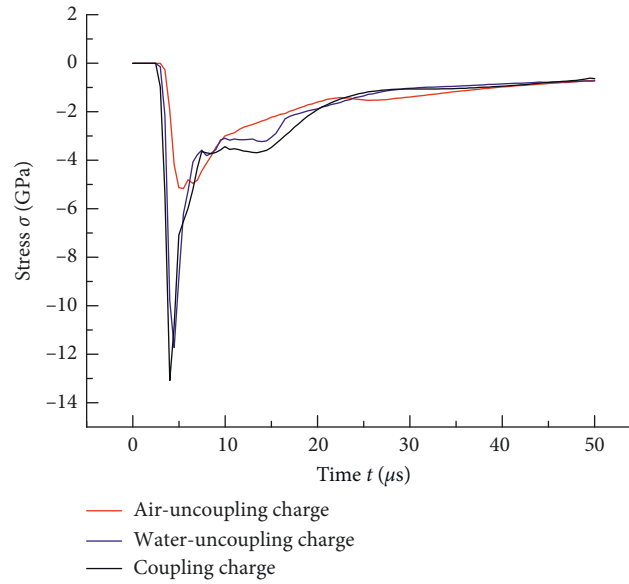

FIGURE 17: Comparison of the pressure of blasting hole wall with different charging methods.

adjacent empty hole in rock blasting, pitch of holes, empty hole diameter, and uncoupled medium are extensively investigated. From the numerical simulation results, we come to the following conclusions.

The stress on adjacent empty hole wall gradually decreases with the increase of the pitch of holes. In the process of stress on empty hole wall changing, the tangential stress is always greater than the radial stress, and the tangential stress peak is usually 3-4 times than the radial stress peak.

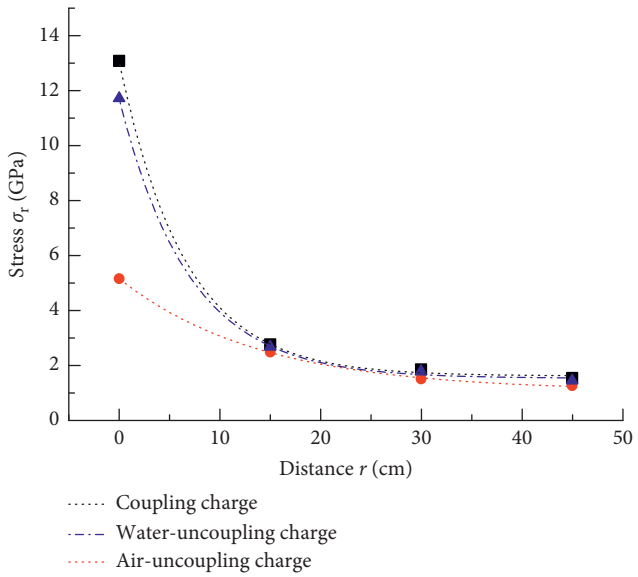

Figure 18: The pressure attenuates in rock with distance.

With the empty hole diameter increasing, the high stress area around the empty hole has a tendency to move towards blasting hole, which indicates that the stress concentration phenomenon weakens and the free surface effect of empty hole plays a major role.

The blasting efficiency of the water-medium uncoupled charging is the highest, and the rock-breaking effect is the best, which is suitable for cut hole blasting. The rock mass damage caused by air-uncoupled charging is minimal. Air medium has a better cushioning effect on the blast wave than the water medium. Air-uncoupled charging can be used in peripheral eye blasting in smooth blasting to reduce the surrounding rock damage.

Data Availability

The data used to support the findings of this study are available from the corresponding author upon request.

Conflicts of Interest

The authors declare that they have no conflicts of interest.

Acknowledgments

This research was funded by the National Natural Science Foundation of China (No. 51375373).

References

[1] J. X. Lai, X. L. Wang, J. L. Qiu, J. Chen, Z. Hu, and H. Wang, "Extreme deformation characteristics and countermeasures for a tunnel in difficult grounds in southern Shaanxi, China," *Environmental Earth Sciences*, vol. 77, p. 706, 2018.

[2] J. L. Qiu, X. L. Wang, S. Y. He, H. Liu, J. Lai, and L. Wang, "The catastrophic landside in Maoxian County, Sichuan, SW China, on June 24, 2017," *Natural Hazards*, vol. 89, no. 3, pp. 1485–1493, 2017.

[3] L. X. Xie, W. B. Lu, Q. B. Zhang, Q. H. Jiang, G. H. Wang, and J. Zhao, "Damage evolution mechanisms of rock in deep tunnels induced by cut blasting," *Tunnelling and Underground Space Technology*, vol. 58, pp. 257–270, 2016.

[4] G. F. Liu, X. T. Feng, G. L. Feng, B. R. Chen, D. F. Chen, and S. Q. Duan, "A method for dynamic risk assessment and management of rockbursts in drill and blast tunnels," *Rock Mechanics and Rock Engineering*, vol. 49, no. 8, pp. 3257–3279, 2016.

[5] J. Lai, K. Wang, J. Qiu, F. Niu, J. Wang, and J. Chen, "Vibration response characteristics of the cross tunnel structure," *Shock and Vibration*, vol. 2016, Article ID 9524206, 16 pages, 2016.

[6] Y. Wang, "Analysis of dynamic characteristics of through-wall cracks between 2 boreholes in the directed fracture controlled blasting," *Fatigue and Fracture of Engineering Materials and Structures*, vol. 41, no. 2, pp. 273–286, 2018.

[7] Z. Y. Wang, C. Fang, Y. L. Chen, and W. Cheng, "A comparative study of delay time identification by vibration energy analysis in millisecond blasting," *International Journal of Rock Mechanics and Mining Sciences*, vol. 60, pp. 389–400, 2013.

[8] A. P. Rustan, "Micro-sequential contour blasting—how does it influence the surrounding rock mass?," *Engineering Geology*, vol. 49, no. 3-4, pp. 303–313, 1998.

[9] M. Li, Z. M. Zhu, R. F. Liu, B. Liu, L. Zhou, and Y. Dong, "Study of the effect of empty holes on propagating cracks under blasting loads," *International Journal of Rock Mechanics and Mining Sciences*, vol. 103, pp. 186–194, 2018.

[10] Z. W. Yue, Y. Guo, P. Xu et al., "Analysis of empty hole effect in directional fracture controlled blastig," *Explosion and Shock Waves*, vol. 35, no. 3, pp. 304–311, 2015.

[11] M. R. Saharan and H. S. Mitri, "Numerical procedure for dynamic simulation of discrete fractures due to blasting," *Rock Mechanics and Rock Engineering*, vol. 41, no. 5, pp. 641–670, 2008.

[12] L. F. Fan, J. W. Gao, Z. J. Wu, S. Q. Yang, and G. W. Ma, "An investigation of thermal effects on micro-properties of granite by X-ray CT technique," *Applied Thermal Engineering*, vol. 140, pp. 505–519, 2018.

[13] J. H. Yang, Q. H. Jiang, Q. B. Zhang, and J. Zhao, "Dynamic stress adjustment and rock damage during blasting excavation in a deep-buried circular tunnel," *Tunnelling and Underground Space Technology*, vol. 71, pp. 591–604, 2018.

[14] S. B. Chai, J. C. Li, Q. B. Zhang, H. B. Li, and N. N. Li, "Stress wave propagation across a rock mass with two non-parallel joints," *Rock Mechanics and Rock Engineering*, vol. 49, no. 10, pp. 4023–4032, 2016.

[15] J. Lai, S. He, J. Qiu et al., "Characteristics of seismic disasters and aseismic measures of tunnels in Wenchuan earthquake," *Environmental Earth Sciences*, vol. 76, p. 94, 2017.

[16] G. W. Ma and X. M. An, "Numerical simulation of blasting-induced rock fractures," *International Journal of Rock Mechanics and Mining Sciences*, vol. 45, no. 6, pp. 966–975, 2008.

[17] W. C. Zhu, J. Wei, J. Zhao, and L. L. Niu, "2D numerical simulation on excavation damaged zone induced by dynamic stress redistribution," *Tunnelling and Underground Space Technology*, vol. 43, pp. 315–326, 2014.

[18] R. J. Qiao, Z. S. Shao, F. Y. Liu, and W. Wei, "Damage evolution and safety assessment of tunnel lining subjected to longduration fire," *Tunnelling and Underground Space Technology*, vol. 83, pp. 354–363, 2019.

[19] N. Vlachopoulos and I. Vazaios, "The numerical simulation of hard rocks for tunnelling purposes at great depths: a comparison between the hybrid FDEM method and continuous

techniques," *Advances in Civil Engineering*, vol. 2018, Article ID 3868716, 18 pages, 2018.

[20] Z. J. Wu, L. F. Fan, Q. S. Liu, and G. Ma, "Micro-mechanical modeling of the macro-mechanical response and fracture behavior of rock using the numerical manifold method," *Engineering Geology*, vol. 225, pp. 49–60, 2016.

[21] R. Ren, S. Xu, Z. Ren et al., "Numerical investigation of particle concentration distribution characteristics in twin-tunnel complementary ventilation system," *Mathematical Problems in Engineering*, vol. 2018, Article ID 1329187, 13 pages, 2018.

[22] Z. N. Zhang and A. Ghassemi, "Simulation of hydraulic fracture propagation near a natural fracture using virtual multidimensional internal bonds," *International Journal for Numerical and Analytical Methods in Geomechanics*, vol. 35, no. 4, pp. 480–495, 2015.

[23] J. F. Liu, H. P. Xie, J. Xu et al., "Discussion on deformation and damping parameters of rock under cyclic loading," *Chinese Journal of Rock Mechanics and Engineering*, vol. 31, no. 4, pp. 770–777, 2012.

[24] C. Z. Qi and Q. H. Qian, "Physical mechanism of dependence of material strength on strain rate for rock-likematerial," *Chinese Journal of Rock Mechanics and Engineering*, vol. 22, no. 2, pp. 177–181, 2003.

[25] K. Hashiba and K. Fukui, "Index of loading-rate dependency of rock strength," *Rock Mechanics and Rock Engineering*, vol. 48, no. 2, pp. 859–865, 2014.

[26] T. J. Wang, "Unified CDM model and local criterion for ductile fracture—I. Unified CDM model for ductile fracture," *Engineering Fracture Mechanics*, vol. 42, no. 1, pp. 177–183, 1992.

[27] P. Vivek and T. G. Sitharam, "Laboratory scale investigation of stress wave propagation and vibrational characteristics in sand when subjected to air-blast loading," *International Journal of Impact Engineering*, vol. 114, pp. 169–181, 2018.

[28] N. Babanouri, H. Mansouri, S. K. Nasab, and M. Bahaadini, "A coupled method to study blast wave propagation in fractured rock masses and estimate unknown properties," *Computers and Geotechnics*, vol. 49, pp. 134–142, 2013.

[29] T. Wang, "A continuum damage model for ductile fracture of weld heat affected zone," *Engineering Fracture Mechanics*, vol. 40, no. 6, pp. 1075–1082, 1991.

[30] R. J. Qiao, Z. S. Shao, W. Wei, and Y. Zhang, "Theoretical investigation into the thermo-mechanical behaviours of tunnel lining during RABT fire development," *Arabian Journal for Science Engineering*, pp. 1–12, 2018.

[31] Z. Q. Wang and Y. Lu, "Numerical analysis on dynamic deformation mechanism of soils under blast loading," *Soil Dynamics and Earthquake Engineering*, vol. 23, no. 8, pp. 705–714, 2015.

[32] X. Z. Li and Z. S. Shao, "Investigation of macroscopic brittle creep failure caused by micro-crack growth under step loading and unloading in rocks," *Rock Mechanics and Rock Engineering*, vol. 49, no. 7, pp. 2581–2593, 2016.

[33] F. L. Fan, Z. J. Wu, Z. Wan, and J. W. Gao, "Experimental investigation of thermal effects on dynamic behavior of granite," *Applied Thermal Engineering*, vol. 125, pp. 94–103, 2017.

[34] T. J. Holmquist, D. W. Templeton, and K. D. Bishnoi, "Constitutive modeling of aluminum nitride for large strain, high-strain rate, and high-pressure application," *International Journal of Impact Engineering*, vol. 25, no. 3, pp. 211–231, 2001.

[35] G. R. Johnson, T. J. Holmquist, and S. R. Beissel, "Response of aluminum nitride (including a phase change) to large strains, high strain rates, and high pressures," *Journal of Applied Physics*, vol. 94, no. 3, pp. 1639–1646, 2003.

[36] Z. L. Wang and Y. C. Li, "Numerical simulation on effects of radial water-decoupling coefficient in engineering blast," *Rock and Soil Mechanics*, vol. 26, no. 12, pp. 1926–1930, 2005.